DOI: 10.1002/ejic.200800348

Spectroscopic and Computational Study on New Blue Emitting $ReL(CO)_3Cl$ Complexes Containing Pyridylimidazo[1,5-*a*]pyridine Ligands

Claudio Garino,[a] Tiziana Ruiu,[a] Luca Salassa,[a] Andrea Albertino,[a] Giorgio Volpi,[a] Carlo Nervi,[a] Roberto Gobetto,*[a] and Kenneth I. Hardcastle[b]

Keywords: Rhenium / X-ray structure / TDDFT / UV/Vis spectroscopy / Luminescence

The structural and photophysical properties of three new $ReL(CO)_3Cl$ complexes (Re**L1**–Re**L3**) and their 1-(2-pyridyl)-imidazo[1,5-*a*]pyridine ligands, namely 3-methyl-1-(2-pyridyl)imidazo[1,5-*a*]pyridine (**L1**), 1-(2-pyridyl)-3-[4-(trifluoromethyl)phenyl]imidazo[1,5-*a*]pyridine (**L2**), and 3-(4-nitrophenyl)-1-(2-pyridyl)imidazo[1,5-*a*]pyridine (**L3**), were studied by spectroscopy, X-ray diffraction, and computational methods. Re**L1**–Re**L3** have high-energy singlet emissions arising from a $\pi \rightarrow \pi^*$ ligand-centered state. In oxygen-free acetonitrile solutions, the complexes display dual fluorescence due to intense ligand-centered triplet emission.

Introduction

The 1-pyridylimidazo[1,5-*a*]pyridine ligands recently received potential interest for optical applications,[1–3] particularly in the field of OLEDs.[4,5] This class of ligands has emission in the blue region of the visible range (450–470 nm), which is a desirable, but critical, feature in OLED technology. In a previous paper[1] we discussed the synthesis and the photophysical properties of new rhenium complexes containing 1-pyridylimidazo[1,5-*a*]pyridine ligands with electron-donor groups on a phenyl substituent. We report here a study on new 1-pyridylimidazo[1,5-*a*]pyridine ligands and their corresponding rhenium complexes (Scheme 1) having electron-withdrawing groups. Comparison between ligands and complexes gave useful insights into their photophysical properties.[6] Time-dependent DFT (TDDFT) calculations on singlet and triplet excited states[7–11] were used to estimate the nature of admixture between metal and ligand orbitals and the character of optically active states.

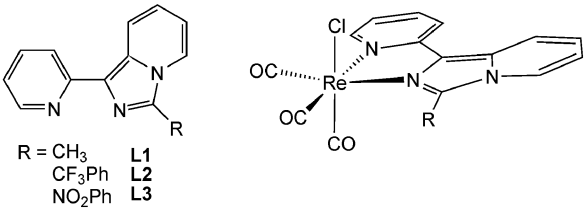

Scheme 1. Schematic representation of the three ligands **L1**–**L3** and the corresponding complexes Re**L1**–Re**L3**.

Results and Discussion

X-ray and Electronic Structure

Crystals of Re**L2** were obtained by solvent (acetonitrile) evaporation. The X-ray structure of Re**L2** (Figure 1) shows the $Re(CO)_3$ unit to be orthogonal but rotated by 13.5° with

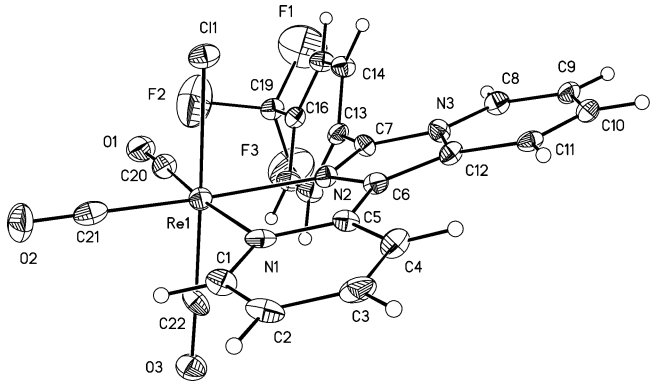

Figure 1. X-ray structure of Re**L2**; displacement ellipsoids are drawn at 30% probability. Selected bond lengths (Å) and angles (°): Re1–C20 1.892(14), Re1–C21 1.897(14), Re1–C22 1.868(13), Re1–N1 2.201(10), Re1–N2 2.185(8), Re1–Cl1 2.520(3), O1–C20–Re1 177.1(10), O2–C21–Re1 178.8(11), O3–C22–Re1 175.5(9), C1–N1–Re1 124.7(8), C5–N1–Re1 117.6(7), C7–N2–Re1 135.5(7), C6–N2–Re1 114.3(6), C22–Re1–C20 88.8(5), C22–Re1–C21 86.1(5), C20–Re1–C21 87.7(5), C22–Re1–N2 99.2(4), C20–Re1–N2 99.1(4), C21–Re1–N2 171.5(4), C22–Re1–N1 91.6(4), C20–Re1–N1 174.0(4), C21–Re1–N1 98.4(4), N2–Re1–N1 74.9(3), C22–Re1–Cl1 176.7(3), C20–Re1–Cl1 93.9(4), C21–Re1–Cl1 92.0(4), N2–Re1–Cl1 82.4(2), N1–Re1–Cl1 86.0(2).

[a] Dipartimento di Chimica IFM, Università di Torino,
Via P. Giuria 7, 10125 Torino, Italy
Fax: +39 011 6707855
E-mail: roberto.gobetto@unito.it
[b] Department of Chemistry, Emory University,
1515 Dickey Drive, Atlanta, Georgia 30322, USA

Supporting information for this article is available on the WWW under http://www.eurjic.org/ or from the author.

respect to the ligand plane of N1–C1–C2–C3–C4–C5; this is due to steric crowding by the pendant (trifluoromethyl)-phenyl substituent, which is rotated with respect to the same plane by 54.3°. Good agreement between X-ray and DFT bond lengths and angles is obtained at the level of calculation employed (see Supporting Information).

The HOMO orbitals of the three ligands have similar features. They consist of π orbitals delocalized on the whole aromatic system. **L2** shows only a little contribution from the trifluoromethyl group. In **L1** and **L2** the LUMO is π* and involves the whole molecule, while in **L3** the orbital surface is centered primarily on the 4-nitrophenyl moiety. In Re**L1**–Re**L3** the HOMO is ligand-centered and has a backdonation contribution from the metal to the pyridylimidazo[1,5-*a*]pyridine rings. The LUMOs of Re**L1** and Re**L2** have small contributions from the Cl and the two equatorial carbonyl groups. As observed for **L3**, the LUMO of Re**L3** is localized on the nitrophenyl ring (with participation from the nitrogen atoms of the imidazole ring).

Absorption and Fluorescence Spectra and Singlet Excited States of L1–L3 and ReL1–ReL3

Absorption and fluorescence spectra were recorded in acetonitrile. Experimental and theoretical data for all investigated compounds are reported in Table 1. The experimental and simulated absorption spectra of **L2** and Re**L2** are shown in Figure 2 together with the emissions. All spectra for the other ligands and complexes are reported in the Supporting Information.

According to TDDFT calculations, the low-energy band of **L1** is a pure π → π*, while the presence of the (trifluoromethyl)phenyl (CF_3Ph) group in **L2** leads to a mixture of a π → π* state and a charge-transfer (CT) state of pyridylimidazo[1,5-*a*]pyridine → CF_3Ph character. Also for **L3** the major band is composed of π → π* and CT (pyridylimidazo[1,5-*a*]pyridine → NO_2Ph) states, as shown by the broad shoulder at 429 nm. Unfortunately, TDDFT underestimates the energy of the CT state of 0.549 eV (100 nm), allowing

Table 1. Absorption and emission properties of **L1**–**L3** and Re**L1**–Re**L3** in acetonitrile.

	λ_{abs} (nm)	ε ($M^{-1}cm^{-1}$)	Trans.	E_{calc} (eV) / (nm)	f[a]	Character	ν_{em}, $\times 10^3$ (cm^{-1}) / (nm)	ϕ	τ_{av} (ns)
L1	368	15400	1	3.40 / 365	0.34	π → π*	21.9 / 457	0.23	8.3
	331	17000	2	3.92 / 317	0.11	π → π*			
	297	13700	3	4.26 / 291	0.23	π → π*			
	279	13300	5	4.87 / 255	0.07	π → π*			
			7	5.38 / 231	0.06	π → π*			
L2	356	14400	1	3.36 / 370	0.46	π → π*	22.1 / 452	0.15	3.6
			2	3.45 / 359	0.29	CT			
	324	13800	3	3.95 / 314	0.15	π → π*/CT			
	295	8300	5	4.28 / 289	0.18	CT (py)			
	230	14100	7	5.03 / 247	0.06	π → π*			
L3	429	18900	1	2.35 / 529	0.43	CT	21.9 / 456	0.004	4.3
	380	21400	2	3.41 / 364	0.28	π → π*			
	328	17600	4	3.96 / 313	0.07	CT			
	268	25600	5	3.98 / 311	0.17	CT (NO_2)			
			7	4.02 / 309	0.16	CT (NO_2)			
			8	4.15 / 299	0.09	CT (NO_2)			
Re**L1**	381	13400	1	3.29 / 377	0.29	π → π*	23.2 / 430	≈ 10^{-4}	9.9
			2	3.49 / 356	0.09	MLCT	17.6 / 568		
			3	3.63 / 342	0.07	MLCT	16.2 / 618		
	310	9400	6	4.17 / 298	0.08	π → π*	14.8 / 675		
			8	4.23 / 293	0.06	MLCT/π → π*			
	275	8900	21	4.94 / 251	0.08	MLCT			
			22	4.97 / 249	0.20	π → π*/LMCT			
Re**L2**	376	15900	1	3.25 / 381	0.24	π → π*	23.4 / 428	0.003	< 3
			2	3.45 / 360	0.17	MLCT	17.9 / 558		
			3	3.56 / 349	0.06	MLCT	16.5 / 605		
	302	14500	4	3.79 / 328	0.06	CT (LC)	15.2 / 660		
			6	3.91 / 317	0.13	π → π*			
			8	4.18 / 297	0.05	MLLCT			
			14	4.35 / 285	0.06	MLCT			
			24	4.77 / 260	0.06	CT(LC)/MLCT			
			27	4.92 / 252	0.09	MLCT			
Re**L3**			1	2.59 / 478	0.14	CT (LC)	21.9 / 456	0.002	10.0
	374	18400	4	3.30 / 375	0.21	MLCT/π → π*	17.9 / 558[b]		
			6	3.49 / 355	0.15	MLCT	16.4 / 608[b]		
			7	3.59 / 346	0.07	MLCT	15.0 / 665[b]		
	306	12700	14	4.20 / 295	0.06	MLLCT			
			16	4.25 / 292	0.08	MLLCT			
	260	20300	22	4.44 / 279	0.09	mixed			
			23	4.53 / 274	0.08	mixed			
			29	4.69 / 265	0.24	MLLCT (NO_2)			

[a] Only electronic transitions with an oscillator strength (f) value higher than 0.05 are reported. [b] Data recorded at 77 K.

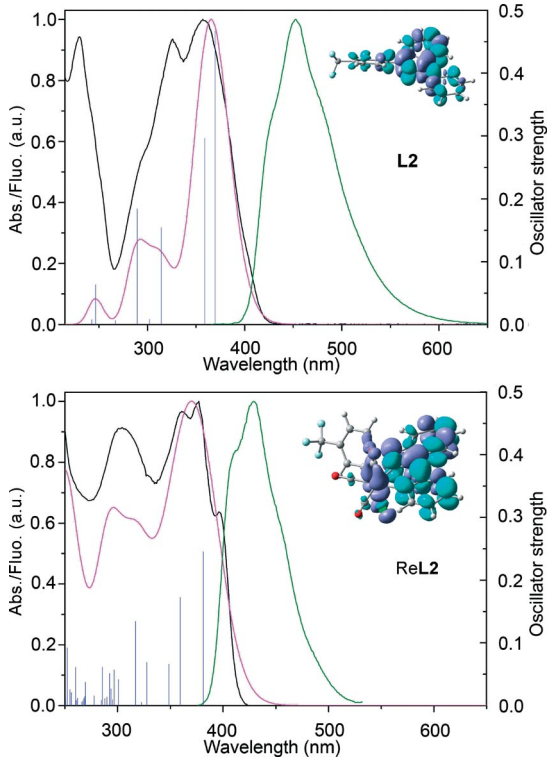

Figure 2. Experimental (black line) and calculated (magenta line) absorption spectra and emission spectrum (green line) for **L2** and Re**L2** in acetonitrile. The singlet excited states are shown as vertical bars with heights equal to the oscillator strength. Inset: Electron density difference maps (EDDMs)[15] of the lowest energy singlet electronic transition for **L2** and Re**L2** (violet indicates a decrease in charge density, while cyan indicates an increase). Theoretical curves and EDDMs were obtained with the program GaussSum 1.05.[16] All spectra were normalized.

only a qualitative interpretation of the absorption spectrum of **L3**.

Re**L1** and Re**L2** have low-energy absorption bands centered at around 380 nm. These bands are both composed of two MLCT (Re → **L1** or **L2**) transitions and a ligand-centered π → π* transition with lower energy. Mixed MLCT and ligand-centered states are present at higher energy (over 300 nm) in the spectrum of Re**L1** and Re**L2**. Re**L3** displays a maximum of absorbance at 374 nm due to a ligand-centered CT state (pyridylimidazo[1,5-*a*]pyridine → NO_2Ph) and two states with MLCT character. Despite a significant error in the energy value of the ligand-centered CT transition (0.545 eV, 83 nm), TDDFT correctly reproduces the blue shift and the decrease in the oscillator strength value for this transition in Re**L3** with respect to **L3**. The complex has, in fact, a less prominent shoulder at 396 nm in the experimental spectrum.

L1 and **L2** both have singlet emission maxima at about 455 nm with lifetimes in the 3–8 ns range and quantum yields of 0.23 and 0.15, respectively. Moreover, they both have narrow bands [FWHM (full width at half maximum) ≈ 3764 cm^{-1}], partially showing vibronic structure. These similarities indicate that, as expected for **L1**, the **L2** emission can be ascribed to a π → π* state centered only on the N-containing rings. In the case of **L3** the position of the band and the modest Stokes shift suggest that the emission also occurs from a π → π* state. Mixing with the low-energy CT state can explain the larger bandwidth (FWHM ≈ 4375 cm^{-1}) and the absence of vibronic structure.

Re**L1**, Re**L2**, and Re**L3** have ligand-based singlet emissions with maxima at 435, 428, and 456 nm respectively. The blue-shifted emission of Re**L1** and Re**L2**, relative to their free ligands, is related to the change in conformation of the ligand (*trans* to *cis*) upon metal coordination.[6] All three complexes, to a large extent, have emitting states with π → π* character. However, the presence of multicomponents in the lifetime decays, the differences in bandwidths and Stokes shifts indicate that other states contribute somehow to the emission. Quantum yields and lifetimes for the three complexes are in agreement with the values measured for other rhenium complexes of this kind.[1] In oxygen-free acetonitrile solutions, three new maxima of decreasing intensity appear at 568, 618, and 675 nm for Re**L1**, and at 558, 605, and 660 nm for Re**L2**; such bands appear only at 77 K for Re**L3** and are centered at 558, 608, and 665 nm. The new bands are due to triplet states since they are red-shifted and strongly dependent on oxygen quenching. The vibrational profile, typical of C=C and C=N stretching (≈ 1425 cm^{-1}), shows that the triplet states have π → π* character. Spin density calculations[12] on the lowest-lying triplet state of Re**L1**–**L3** confirm this assignment (see Figure 3 for Re**L2**). Emission energies calculated with the ΔSCF approach[13,14] are slightly lower than the experimental ones; they are 693 nm for both Re**L1** and Re**L2** and 685 nm for Re**L3**.

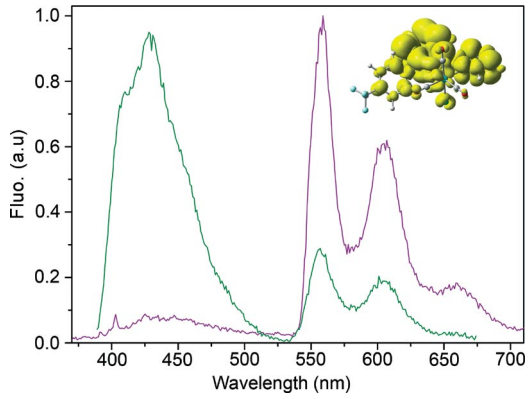

Figure 3. Emission spectra of Re**L2** in the deoxygenated acetonitrile solution at room temperature (green line) and at 77 K (purple line). Inset: Plots of the spin density (isovalue 0.0004) of the lowest lying triplet state geometry of complex Re**L2**. All spectra were normalized.

Conclusions

The 1-pyridylimidazo[1,5-*a*]pyridine ligands are good candidates for preparing blue-emitting metal complexes, although Re**L1**–Re**L3** have low quantum yields. Modification of substituents in position 3 can be achieved easily by

straightforward synthetic procedures that allow tuning of the photophysical properties of the complex. The rhenium compounds investigated in this work present singlet/triplet dual emission in the absence of oxygen. In all cases, the nature of the emissive state is a ligand-centered $\pi \rightarrow \pi^*$ transition, even if, according to TDDFT, CT character contributes to the emission. **L3** and Re**L3** do not present pure CT state emissions, despite the presence of a strong electron-withdrawing group such as nitrophenyl. Pure CT states were observed for the analogous dimethylaminophenyl derivatives.[1] In Re**L3** the metal core and the nitrophenyl group compete for the electron density localized on the 1-pyridylimidazo[1,5-*a*]pyridine moiety. In the dimethylaminophenyl analogue, on the contrary, metal coordination favors electron density migration from the dimethylaminophenyl group to the chelated rings. Finally, it is worth noting that an increase in the level of calculation for **L3** and Re**L3** (B3LYP/6-311G** and B3LYP/LanL2DZ/6-311G**, respectively) does not provide any significant improvement in the prevision of the singlet state energies.

Experimental Section

Physical Methods: NMR spectra were recorded with a JEOL EX 400 spectrometer (B_0 = 9.4 T, ^{1}H operating frequency: 399.78 MHz) with chemical shifts referenced to residual protons in the solvent ([D_6]acetone and [D_6]dmso). UV/Vis absorption spectra were measured with a double-beam Perkin–Elmer Lambda 20 UV/Vis spectrophotometer equipped with a 1-cm quartz cell. Emission spectra as well as luminescence lifetimes were obtained by using a HORIBA Jobin Yvon IBH Fluorolog-TCSPC spectrofluorimeter. Fluorescence quantum yields were determined by using quinine bisulfate (0.1 N H_2SO_4) as standard (ϕ = 0.546[17]). Luminescence lifetimes were determined by time-correlated single-photon counting. The data were collected into 2048 channels to 10,000 counts in the peak channel. Emission decay data were analyzed with the software DAS6 (TCSPC Decay Analysis Software). Mass spectra were recorded by using an XCT PLUS electrospray ionization–ion trap (ESI–IT) mass spectrometer (Agilent Italy, Milan). Samples were dissolved in methanol/water (9:1) solution with formic acid (0.1%). The *m*/*z* scan range was 200–800.

X-Ray Structure Determination: A suitable crystal of [Re{1-(2-pyridyl)-3-[4-(trifluoromethyl)phenyl]imidazo[1,5-*a*]pyridine}$(CO)_3$Cl] (Re**L2**) was coated with Paratone N oil, suspended in a small fiber loop, and placed in a cooled nitrogen gas stream at 173 K on a Bruker D8 SMART APEX CCD sealed tube diffractometer with graphite monochromated Mo-K_α (0.71073 Å) radiation. Data were measured by using a series of combined phi and omega scans with 10 s frame exposures and 0.3° frame widths. Data collection, indexing, and initial cell refinements were all carried out with SMART[18] software. Frame integration and final cell refinements were performed with SAINT[19] software. The final cell parameters were determined from least-squares refinement on 5171 reflections. The SADABS[20] program was used to carry out absorption corrections. The structure was solved by direct methods and difference Fourier techniques (SHELXTL, V6.12).[21] Hydrogen atoms were placed into their expected chemical positions by using the HFIX command and were included in the final cycles of least-squares with isotropic U_{ij} values related to the atoms that were ridden upon. All non-hydrogen atoms were refined anisotropically. Structure solution, refinement, graphics, and generation of publication materials were performed by using SHELXTL, V6.12 software. CCDC-683746 contains the supplementary crystallographic data for Re**L2**. This data can be obtained free of charge from The Cambridge Crystallographic Data Centre via www.ccdc.cam.ac.uk/data_request/cif.

Computational Details: Gaussian 03[22] was employed for all calculations. Geometry optimization of the ground and lowest-lying triplet state in the gas phase were performed with the B3LYP functional.[23,24] The LanL2DZ/6-31G** basis set was used for the complexes, while the ligands were optimized at the B3LYP/6-31G** level. The nature of all stationary points was confirmed by performing a normal-mode analysis. Eight singlet excited states for **L1**–**L3** and thirty-two singlet excited states for Re**L1**–Re**L3** were obtained with time-dependent DFT (TDDFT) calculations[25,26] and the conductor-like polarizable continuum model method (CPCM)[27–29] with acetonitrile as solvent.

Synthesis of Ligands: All ligands were prepared according to a published procedure;[30] only **L1** was obtained with a slight modification of such a procedure.

3-Methyl-1-(2-pyridyl)imidazo[1,5-*a*]pyridine (L1): A mixture of 2,2′-dipyridyl ketone (1.84 g, 10.0 mmol), acetaldehyde (0.88 g, 20.0 mmol), and ammonium acetate (3.86 g, 50.0 mmol) in glacial acetic acid (100 mL) was stirred at 110 °C under nitrogen. After 5 h, the reaction mixture was cooled to room temperature, and the acetic acid was removed by evaporation under vacuum. The solid was dissolved in an aqueous solution of NaCl and $NaHCO_3$, and the mixture was extracted with CH_2Cl_2. The organic layer was separated, and the solvent was evaporated under vacuum. The formed solid was extracted with petroleum ether, and then the solvent was removed by evaporation under vacuum. Yield 38% (0.80 g). ^{1}H NMR (400 MHz, [D_6]dmso, 298 K): δ = 2.65 (s, 3 H), 6.74 (t, $^3J_{HH}$ = 6.8 Hz, 1 H), 6.96 (t, $^3J_{HH}$ = 9.2 Hz, 1 H), 7.12 (t, $^3J_{HH}$ = 6.2 Hz, 1 H), 7.76 (t, $^3J_{HH}$ = 9.5 Hz, 1 H), 8.01 (d, $^3J_{HH}$ = 8.0 Hz, 1 H), 8.17 (d, $^3J_{HH}$ = 7.2 Hz, 1 H), 8.46 (d, $^3J_{HH}$ = 9.2 Hz, 1 H), 8.55 (d, $^3J_{HH}$ = 4.7 Hz, 1 H) ppm. ^{13}C NMR (100 MHz, [D_6]dmso, 298 K): δ = 12.3, 112.9, 118.6, 120.0, 120.3, 120.8, 122.5, 127.4, 128.4, 135.5, 136.4, 149.0, 154.9 ppm.

1-(2-Pyridyl)-3-[4-(trifluoromethyl)phenyl]imidazo[1,5-*a*]pyridine (L2): Yield 77% (2.6 g). ^{1}H NMR (400 MHz, [D_6]acetone, 298 K): δ = 6.90 (t, $^3J_{HH}$ = 8.6 Hz, 1 H), 7.10 (t, $^3J_{HH}$ = 8.6 Hz, 1 H), 7.19 (t, $^3J_{HH}$ = 6.0 Hz, 1 H), 7.82 (t, $^3J_{HH}$ = 9.1 Hz, 1 H), 7.93 (d, $^3J_{HH}$ = 7.9 Hz, 2 H), 8.21 (d, $^3J_{HH}$ = 6.6 Hz, 2 H), 8.26 (d, $^3J_{HH}$ = 8.5 Hz, 1 H), 8.63 (d, $^3J_{HH}$ = 5.9 Hz, 2 H), 8.78 (d, $^3J_{HH}$ = 9.8 Hz, 1 H) ppm. ^{13}C NMR (100 MHz, [D_6]acetone, 298 K): δ = 115.5, 120.3, 121.5, 122.5, 122.7, 123.2, 126.6, 126.7, 129.4, 130.2, 130.5, 131.7, 135.1, 137.0, 137.1, 149.9, 156.0 ppm.

3-(4-Nitrophenyl)-1-(2-pyridyl)imidazo[1,5-*a*]pyridine (L3): Yield 84% (2.7 g). ^{1}H NMR (400 MHz, [D_6]acetone, 298 K): δ = 6.98 (t, $^3J_{HH}$ = 7.6 Hz, 1 H), 7.17 (t, $^3J_{HH}$ = 10.1 Hz, 1 H), 7.22 (t, $^3J_{HH}$ = 8.6 Hz, 1 H), 7.85 (t, $^3J_{HH}$ = 9.4 Hz, 1 H), 8.30 (m, 3 H), 8.45 (d, $^3J_{HH}$ = 13.8 Hz, 2 H), 8.45 (d, $^3J_{HH}$ = 6.6 Hz, 1 H), 8.75 (d, $^3J_{HH}$ = 7.2 Hz, 1 H), 8.83 (d, $^3J_{HH}$ = 10.4 Hz, 1 H) ppm. ^{13}C NMR (100 MHz, [D_6]acetone, 298 K): δ = 115.9, 120.5, 121.7, 122.5, 123.3, 123.6, 125.1, 129.3, 137.2, 150.0 ppm.

General Synthesis of *fac*-Re(L)$(CO)_3$Cl: Chlorido complexes, Re(L)$(CO)_3$Cl, were obtained with a slight modification of a previously published procedure;[31] $Re(CO)_5Cl$ (0.40 g, 1.1 mmol) was heated at reflux with equimolar quantities of the appropriate ligand in toluene for 4 h. The yellow products were precipitated from solution, then filtered, and washed with toluene and ethyl ether.

***fac*-ReL1(CO)$_3$Cl (ReL1):** Yield 77% (0.44 g). ^{1}H NMR (400 MHz, [D$_6$]dmso, 298 K): δ = 2.98 (s, 3 H), 7.14 (t, $^3J_{HH}$ = 7.0 Hz, 1 H), 7.40 (m, 2 H), 8.13 (t, $^3J_{HH}$ = 7.9 Hz, 1 H), 8.37 (m, 2 H), 8.50 (d, $^3J_{HH}$ = 7.2 Hz, 1 H), 8.88 (d, $^3J_{HH}$ = 5.6 Hz, 1 H) ppm. ^{13}C NMR (100 MHz, [D$_6$]dmso, 298 K): δ = 13.3, 115.1, 117.1, 120.4, 123.1, 124.5, 125.5, 128.6, 129.2, 135.5, 139.5, 139.7, 152.4, 190.1, 197.9, 198.0 ppm. MS (ESI): *m*/*z* = 512 [M – Cl + CH_3OH]$^+$, 480 [M – Cl]$^+$. $C_{16}H_{11}ClN_3O_3Re$ (514.94): calcd. C 37.32, H 2.15, N 8.16; found C 37.19, H 2.01, N 8.04.

***fac*-ReL2(CO)$_3$Cl (ReL2):** Yield 81% (0.58 g). ^{1}H NMR (400 MHz, [D$_6$]dmso, 298 K): δ = 7.10 (t, $^3J_{HH}$ = 6.9 Hz, 1 H), 7.48 (t, $^3J_{HH}$ = 6.9 Hz, 1 H), 7.50 (t, $^3J_{HH}$ = 6.7 Hz, 1 H), 8.09 (m, 4 H), 8.21 (m, 2 H), 8.50 (d, $^3J_{HH}$ = 2.3 Hz, 1 H), 8.52 (d, $^3J_{HH}$ = 4.1 Hz, 1 H), 8.90 (d, $^3J_{HH}$ = 5.6 Hz, 1 H) ppm. ^{13}C NMR (100 MHz, [D$_6$]-dmso, 298 K): δ = 116.3, 117.2, 120.9, 121.7, 123.6, 124.3, 125.2, 126.2, 126.6, 129.2, 129.4, 130.5, 131.1, 131.4, 132.3, 138.8, 139.8, 152.3, 152.7, 190.1, 195.8, 197.7 ppm. MS (ESI): *m*/*z* = 642 [M – Cl + CH_3OH]$^+$, 610 [M – Cl]$^+$. $C_{22}H_{12}ClF_3N_3O_3Re$ (645.01): calcd. C 40.97, H 1.88, N 6.51; found C 41.11, H 1.97, N 6.39.

***fac*-ReL3(CO)$_3$Cl (ReL3):** Yield 73% (0.50 g). ^{1}H NMR (400 MHz, [D$_6$]dmso, 298 K): δ = 7.13 (t, $^3J_{HH}$ = 6.74 Hz, 1 H), 7.50 (m, 2 H), 8.18 (d, $^3J_{HH}$ = 8.8 Hz, 2 H), 8.22 (t, $^3J_{HH}$ = 7.9 Hz, 1 H), 8.25 (d, $^3J_{HH}$ = 7.2 Hz, 1 H), 8.52 (m, 2 H), 8.58 (d, $^3J_{HH}$ = 8.8 Hz, 2 H), 8.91 (d, $^3J_{HH}$ = 5.3 Hz, 1 H) ppm. ^{13}C NMR (100 MHz, [D$_6$]dmso, 298 K): δ = 116.4, 117.3, 120.9, 123.7, 124.2, 126.8, 129.4, 129.7, 132.7, 133.1, 138.1, 139.9, 149.0, 152.2, 152.8, 190.0, 196.1, 197.6 ppm. MS (ESI): *m*/*z* = 619 [M – Cl + CH_3OH]$^+$, 587 [M – Cl]$^+$. $C_{21}H_{12}ClN_4O_5Re$ (622.01): calcd. C 40.55, H 1.94, N 9.01; found C 40.68, H 2.05, N 8.82.

Supporting Information (see footnote on the first page of this article): calculated and experimental UV/Vis spectra, emission spectra, electron density difference maps (EDDMs), singlet transition energies for **L1**, **L3**, Re**L1** and Re**L3**, selected bond lengths for Re**L1**–Re**L3**, and triplet spin density plots for Re**L1** and Re**L3**.

Acknowledgments

The authors acknowledge financial support of this work by Regione Piemonte.

[1] L. Salassa, C. Garino, A. Albertino, G. Volpi, C. Nervi, R. Gobetto, K. I. Hardcastle, *Organometallics* **2008**, *27*, 1427–1435.
[2] A. G. Ligtenbarg, A. L. Spek, R. Hage, B. L. Feringa, *J. Chem. Soc., Dalton Trans.* **1999**, 659–661.
[3] M. E. Bluhm, M. Ciesielski, W. O. Görls, M. Döring, *Inorg. Chem.* **2003**, *42*, 8878–8885.
[4] P.-T. Chou, Y. Chi, *Chem. Eur. J.* **2007**, *13*, 380–395.
[5] P.-T. Chou, Y. Chi, *Eur. J. Inorg. Chem.* **2006**, 3319–3332.
[6] C. Garino, R. Gobetto, C. Nervi, L. Salassa, E. Rosenberg, J. B. A. Ross, X. Chu, K. I. Hardcastle, C. Sabatini, *Inorg. Chem.* **2007**, *46*, 8752–8762.
[7] F. De Angelis, S. Fantacci, N. Evans, C. Klein, S. M. Zakeeruddin, J. E. Moser, K. Kalyanasundaram, H. J. Bolink, M. Gratzel, M. K. Nazeeruddin, *Inorg. Chem.* **2007**, *46*, 5989–6001.
[8] C. Dragonetti, L. Falciola, P. Mussini, S. Righetto, D. Roberto, R. Ugo, A. Valore, F. De Angelis, S. Fantacci, A. Sgamellotti, M. Ramon, M. Muccini, *Inorg. Chem.* **2007**, *46*, 8533–8547.
[9] F. De Angelis, S. Fantacci, A. Sgamellotti, E. Cariati, R. Ugo, P. C. Ford, *Inorg. Chem.* **2006**, *45*, 10576–10584.
[10] S. Fantacci, F. De Angelis, A. Selloni, *J. Am. Chem. Soc.* **2003**, *125*, 4381–4387.
[11] A. Albertino, C. Garino, S. Ghiani, R. Gobetto, C. Nervi, L. Salassa, E. Rosenberg, A. Sharmin, G. Viscardi, R. Buscaino, M. Milanesio, G. Croce, *J. Organomet. Chem.* **2006**, *692*, 1377–1391.
[12] A. Vlček Jr, S. Záliš, *Coord. Chem. Rev.* **2007**, *251*, 258–287.
[13] T. Ziegler, A. Rauk, E. J. Baerends, *Theor. Chim. Acta* **1977**, *43*, 261–271.
[14] C. Daul, *Int. J. Quantum Chem.* **1994**, *52*, 867–877.
[15] W. R. Browne, N. M. O'Boyle, J. J. McGarvey, J. G. Vos, *Chem. Soc. Rev.* **2005**, *34*, 641–663.
[16] N. M. O'Boyle, J. G. Vos, GaussSum 1.0, Dublin City University, **2005**. Available at http://gausssum.sourceforge.net.
[17] D. F. Eaton, *Pure Appl. Chem.* **1988**, *60*, 1107–1114.
[18] SMART Version 5.628, Bruker AXS, Inc., 5465 East Cheryl Parkway, Madison, WI 53711-5373, USA, **2003**.
[19] SAINT Version 6.36A, Bruker AXS, Inc., 5465 East Cheryl Parkway, Madison, WI 53711-5373, USA, **2002**.
[20] G. M. Sheldrick, SADABS Version 2.10, University of Göttingen, Germany, **2003**.
[21] SHELXTL V6.12, Bruker AXS, Inc., 5645 East Cheryl Parkway, Madison, WI 53711-5373, USA, **2002**.
[22] M. J. Frisch, G. W. Trucks, H. B. Schlegel, G. E. Scuseria, M. A. Robb, J. R. Cheeseman, J. A. Montgomery Jr, T. Vreven, K. N. Kudin, J. C. Burant, J. M. Millam, S. S. Iyengar, J. Tomasi, V. Barone, B. Mennucci, Cossi, M, G. Scalmani, N. Rega, G. A. Petersson, H. Nakatsuji, M. Hada, M. Ehara, K. Toyota, R. Fukuda, J. Hasegawa, M. Ishida, T. Nakajima, Y. Honda, O. Kitao, H. Nakai, M. Klene, X. Li, J. E. Knox, H. P. Hratchian, J. B. Cross, C. Adamo, J. Jaramillo, R. Gomperts, R. E. Stratmann, O. Yazyev, A. J. Austin, R. Cammi, C. Pomelli, J. Ochterski, P. Y. Ayala, K. Morokuma, G. A. Voth, P. Salvador, J. J. Dannenberg, V. G. Zakrzewski, S. Dapprich, A. D. Daniels, M. C. Strain, O. Farkas, D. K. Malick, A. D. Rabuck, K. Raghavachari, J. Forestman, B, J. V. Ortiz, Q. Cui, A. G. Baboul, S. Clifford, J. Cioslowski, B. B. Stefanov, G. Liu, A. Liashenko, P. Piskorz, I. Komaromi, R. L. Martin, D. J. Fox, T. Keith, M. A. Al-Laham, C. Y. Peng, A. Nanayakkara, M. Challacombe, P. M. W. Gill, B. Johnson, W. Chen, M. W. Wong, C. Gonzales, J. A. Pople, *Gaussian 03*, revision C.02, Gaussian Inc., Wallingford CT, **2004**.
[23] A. D. Becke, *J. Chem. Phys.* **1993**, *98*, 5648–5652.
[24] C. Lee, W. Yang, R. G. Parr, *Phys. Rev. B: Condens. Matter* **1988**, *37*, 785–789.
[25] M. E. Casida, C. Jamorski, K. C. Casida, D. R. Salahub, *J. Chem. Phys.* **1998**, *108*, 4439–4449.
[26] R. E. Stratmann, G. E. Scuseria, M. J. Frisch, *J. Chem. Phys.* **1998**, *109*, 8218–8224.
[27] V. Barone, M. Cossi, *J. Phys. Chem. A* **1998**, *102*, 1995–2001.
[28] M. Cossi, N. Rega, G. Scalmani, V. Barone, *J. Comput. Chem.* **2003**, *24*, 669–681.
[29] M. Cossi, V. Barone, *J. Chem. Phys.* **2001**, *115*, 4708–4717.
[30] J. Wang, L. Dyers, R. Mason, P. Amoyaw, X. R. Bu, *J. Org. Chem.* **2005**, *70*, 2353–2356.
[31] J. V. Caspar, T. J. Meyer, *J. Phys. Chem. A* **1983**, *87*, 952–957.

Received: April 4, 2008
Published Online: May 28, 2008

